This paper is available on line at http://www.mcponline.org

Structural and Quantitative Evidence for Dynamic Glycome Shift on Production of Induced Pluripotent Stem Cells*[S]

Kayo Hasehira‡, Hiroaki Tateno‡, Yasuko Onuma§, Yuzuru Ito§, Makoto Asashima§, and Jun Hirabayashi‡¶

We recently reported that induced pluripotent stem cells (iPSCs) prepared from different human origins acquired similar glycan profiles to one another as well as to human embryonic stem cells. Although the results strongly suggested attainment of specific glycan expressions associated with the acquisition of pluripotency, the detailed glycan structures remained to be elucidated. Here, we perform a quantitative glycome analysis targeting both *N*- and *O*-linked glycans derived from 201B7 human iPSCs and human dermal fibroblasts as undifferentiated and differentiated cells, respectively. Overall, the fractions of high mannose-type *N*-linked glycans were significantly increased upon induction of pluripotency. Moreover, it became evident that the type of linkage of Sia on *N*-linked glycans was dramatically changed from α-2–3 to α-2–6, and the expression of α-1–2 fucose and type 1 LacNAc structures became clearly apparent, while no such glycan epitopes were detected in fibroblasts. The expression profiles of relevant glycosyltransferase genes were fully consistent with these results. These observations indicate unambiguously the manifestation of a "glycome shift" upon conversion to iPSCs, which may not merely be the result of the initialization of gene expression, but could be involved in a more aggressive manner either in the acquisition or maintenance of the undifferentiated state of iPSCs. *Molecular & Cellular Proteomics 11: 10.1074/mcp.M112.020586, 1913–1923, 2012.*

Induced pluripotent stem cells (iPSCs)[1] are genetically manufactured pluripotent cells obtained by the transfection of reprogramming factors. Such iPSCs were first reported in 2006 for the mouse (1) and in 2007 for humans (2, 3). Although iPSCs have already been used in the fields of drug development and disease models (4–7), basic aspects of iPSCs largely remain to be elucidated to provide us with a fuller understanding of their properties and for therapeutic applications to be developed in the field of regenerative medicine. These aspects include the need for a definitive system to be established to evaluate their properties; *e.g.* pluripotency, differentiation propensity, risk of possible contamination of xenoantigens, and even the potential for tumorigenesis. Cell surface glycans are often referred to as the "cell signature," which changes dramatically depending on the cell properties and conditions (8) as a result of changes in gene expression, including epigenetic modifications of glycan-related molecules. Glycans, because of their outermost cell-surface locations and structural complexity, are considered to be most advantageous communication molecules, playing roles in various biological phenomena. Indeed, SSEA3/4 and Tra-1–60/81, which have been used to discriminate pluripotency, are cell surface glycan epitopes that respond to some specific antibodies (9–12).

Glycan-mediated cell-to-cell interactions have been shown to play important roles in various biological phenomena including embryogenesis and carcinogenesis (13–16). This might also be the case for the acquisition and maintenance of iPSC and ESC pluripotency, although there remains much to clarify concerning the roles of cell surface glycans in these events. Thus, the development of novel cell surface markers to evaluate the properties of iPSCs and ESCs is keenly required. Toward this goal, a glycomic approach has been made by several groups (17–20). In our previous study using an advanced lectin microarray technique (21), thirty-eight lectins capable of discriminating between iPSCs and SCs were statistically selected, and the characteristic features of the pluripotent state were obtained. The glycan profiles of the parent SCs, derived from four different tissues, were totally different from one another and from those of the iPSCs. Despite this observation, the technique used lacks the ability

From the ‡Research Center for Stem Cell Engineering, National Institute of Advanced Industrial Science and Technology (AIST), Central 2, 1-1-1 Umezono, Tsukuba, Ibaraki 305-8568, Japan; §Research Center for Stem Cell Engineering, National Institute of Advanced Industrial Science and Technology (AIST), Tsukuba Central 4, 1-1-1 Higashi, Tsukuba, Ibaraki 305-8562, Japan

Received May 18, 2012, and in revised form, September 4, 2012
Published, MCP Papers in Press, September 27, 2012, DOI 10.1074/mcp.M112.020586

[1] The abbreviations used are: iPSC, induced pluripotent stem cell; Fuc, fucose; Gal, D-galactose; GalNAc, *N*-acetyl-D-galactosamine; Glc, D-glucose; GlcNAc, *N*-acetyl-D-glucosamine; HPLC, high performance liquid chromatography; LacNAc, N-acetyllactosamine; Man, D-mannose; MALDI, matrix-assisted laser desorption-ionization; MS, mass spectrometry; NeuAc, *N*-acetylneuraminic acid; PA-, pyridylaminated; SC, somatic cell; Sia, sialic acid; TOF, time of flight.

to determine detailed glycan structures or allow their quantification. For this purpose, a conventional approach based on high performance liquid chromatography (HPLC) combined with matrix-assisted laser desorption-ionization (MALDI) - time of flight (TOF) mass spectrometry (MS) was undertaken for both the definitive identification of glycan structures and their quantitative comparison, which remained unclear in the previous analysis (21).

We report here structural data on *N*-linked and *O*-linked glycans derived from the human iPSC 201B7 cell line (2) and human dermal fibroblasts (SC) representing undifferentiated and differentiated cells, respectively. For quantitative comparison, the glycans were liberated by gas-phase hydrazinolysis from similar numbers of cells (22–25) fluorescently tagged with 2-aminopyridine (2-AP) at their reducing terminus (26, 27), following which the derived pyridylaminated (PA-) glycans were purified by multiple-mode (*i.e.* anion-exchange, size-fractionation and reverse-phase) HPLC. Their structures were determined and quantified by HPLC mapping assisted with MALDI-TOF-MS and exoglycosidase digestion analyses. This report thus provides the first structural evidence showing the occurrence of a dynamic "glycome shift" upon induction of pluripotency.

EXPERIMENTAL PROCEDURES

Cells—As representative iPSCs, 201B7 cells, the first iPSCs established from human dermal fibroblasts by the Yamanaka group, were used (2). The cells were maintained in DMEM-F12 medium (Invitrogen) supplemented with 20% knockout serum replacement (KSR: Invitrogen), 0.1 mM 2-mercaptoethanol (Sigma-Aldrich), MEM non-essential amino acids (Invitrogen) and 10 ng/ml recombinant human basic FGF (Wako, Osaka, Japan) on mitomycin C-treated mouse embryo fibroblast feeder cells. As a counterpart SC, we chose normal human dermal fibroblasts (American Type Culture Collection: ATCC), which were maintained in fibroblast basal medium (ATCC) supplemented with fibroblast growth kit-low serum (ATCC) containing recombinant human (rh-) FGFβ (final concentration: 5 ng/ml), L-glutamine (7.5 mM), ascorbic acid (50 μg/ml), hydrocortisone hemisuccinate (1 μg/ml), rh-insulin (5 μg/ml) and fetal bovine serum (2%). For both differentiated fibroblasts (SC) and undifferentiated 201B7 (iPS) cells, two separate cultures of the same quantities were prepared for quantitative structural analysis.

Materials—2-AP was obtained from Wako (Osaka, Japan). Anhydrous hydrazine (Hydraclub hydrazinolysis reagent Y) was purchased from J-Oil Mills, Inc. (Tokyo, Japan), and Dowex 50WX2 (200- 400 mesh, H^+ form) was from Muromachi Technos Co., Ltd (Tokyo, Japan). The Sep-PAK Plus C18 cartridge was from Waters (Beverly, MA). The Mono Q 5/5 HR column (5.0 $\times$ 50 mm), the PALPAK Type-R column (4.6 $\times$ 250 mm) and the Shodex Asahipak NH2P-50 4D column (4.6 $\times$ 150 mm) were from GE Healthcare Bio-Sciences Corp. (Piscataway, NJ), Takara Bio (Shiga, Japan), and Showa Denko (Tokyo, Japan), respectively. α-2–3,-6 sialidase (*Clostridium perfringens*) and β-1–3-galactosidase (*Xanthomonas manihotis*, recombinant, *Escherichia coli*) were from Merck (Darmstadt, Germany). β-galactosidase (Jack bean), β-*N*-acetylhexosaminidase (Jack bean), and α-mannosidase (Jack bean) were from Seikagaku Co. (Tokyo, Japan). α-1–2 L-fucosidase (*Corynebacterium* sp.) and α-2–3 sialidase cloned from *Salmonella typhimurimum* LT2 and expressed in *E. coli* was from Takara Bio (Shiga, Japan). α-L fucosidase (bovine kidney) was from ProZyme, Inc. (California, US). 2, 5-hydroxybenzoic acid was from Bruker Daltonics (Billerica, MA). Acetonitrile and 1-butanol were of HPLC grade, while the other chemicals were of analytical grade.

Release of N- and O-linked Glycans and Pyridylamination—Protein glycans were released from iPSC and SC by the established method for gas-phase hydrazinolysis (22–25). Each group of cells ($\sim$1 $\times$ 10^7cells) was extensively lyophilized *in vacuo* in a single tube, and treated with anhydrous hydrazine at 100 °C for 4 h using Hydraclub Y2100 (J-Oil Mills, Inc., Tokyo, Japan). After the reaction, the anhydrous hydrazine was removed *in vacuo*. The released glycans were re-*N*-acetylated, desalted with Dowex 50WX2, and lyophilized (22). The glycans thus obtained were pyridylaminated using 0.02 ml of coupling reagent and 0.07 ml of freshly prepared reducing reagent as described previously (26, 27). The bulk of excess reagents in the reaction mixture was removed by phenol/chloroform extraction (28) and subsequent solid-phase extraction using a Sep-PAK Plus C18 cartridge (29). The pyridylaminated (PA) glycans were analyzed by HPLC.

HPLC—Anion-exchange HPLC was performed on a Mono-Q column at a flow rate of 1.0 ml/min using two eluents, A and B. Eluent A was distilled water titrated to pH 9.0 with 1 M aqueous ammonia and eluent B was a 0.5 M ammonia acetate solution titrated to pH 9.0. The column was equilibrated with 100% eluent A. After injecting a sample, the proportion (v/v) of eluent B was increased linearly to 10% (3 min), then to 40% (14 min), and finally to 100% (5 min). The fluorescence of the eluted PA-glycans was detected with excitation and emission wavelengths of 310 nm and 380 nm, respectively.

Size-fractionation HPLC was performed on a Shodex Asahipak NH2P-50 4D column (4.6 $\times$ 150 mm) at a flow rate of 1.0 ml/min at 25 °C with a gradient system: two eluents, C and D, were used, where eluent C was acetonitrile/water:acetic acid (970:70:3, v/v/v) titrated to pH 7.0 with 7 M aqueous ammonia, whereas eluent D was acetonitrile/water/acetic acid (200:800:3, v/v/v) titrated to pH 7.0 with 7 M aqueous ammonia. The column was equilibrated with 95% eluent C and 5% eluent D. After injection of a sample solution, the proportion (v/v) of eluent D was increased linearly from 5% to 33% (3 min), and to 100% (75 min). The fluorescence of the glycans was detected with excitation and emission wavelengths of 320 nm and 400 nm, respectively.

Reversed-phase HPLC was performed on a PALPAK Type-R column (4.6 $\times$ 250 mm) with two eluents, E and F, where eluent E was 100 mM ammonium acetate, pH 4.0, and eluent F was 100 mM ammonium acetate, pH 4.0, containing 0.5% (v/v) 1-butanol. The column was equilibrated with 75% eluent E and 25% eluent F. After injection of a sample, the proportion (v/v) of eluent F was increased linearly from 25% to 100% (60 min) at a flow rate of 1.0 ml/min at 25 °C. The fluorescence of the glycans was detected with excitation and emission wavelengths of 320 nm and 400 nm, respectively.

MS—PA-glycans purified with yields of 1 pmol or more were subjected to subsequent analysis by MALDI-TOF-MS with an Ultraflex mass spectrometer (Bruker Daltonics, Bremen, Germany), equipped with a 337-nm nitrogen laser, and set at 20 kV extraction voltage. 2, 5-Dihydroxybenzoic acid (1 mg/ml in 30% ethanol) was used as the matrix. Analyses were carried out in reflector mode over a mass range of *m/z* 0 to 2000 in the positive ion mode. Each spectrum was measured by 150 laser shots.

Quantification of PA-saccharides—Each of the PA-glycans was quantified as the average of two separate experiments by the peak area in comparison with that corresponding to an appropriate authentic standard under the same HPLC conditions. PA-GlcNAc was used as the authentic calibration standard. Relative yields were expressed as percentages compared with the total amounts of *N*-linked or *O*-linked glycans prepared from each of the iPSC and SC samples.

Exoglycosidase Treatment—Exoglycosidase treatment of PA-glycans was carried out by using α-2–3,-6 sialidase (*Clostridium perfrin-*

gens: Merck), α-2–3 sialidase (*Salmonella typhimurimum* LT2, recombinant, *Escherichia coli*: Takara Bio), β-galactosidase (Jack bean: Seikagaku Co.), β-1–3 galactosidase (*Xanthomonas manihotis*, recombinant, *Escherichia coli*: Merck), β-*N*-acetylhexosaminidase (Jack bean: Seikagaku Co.), α-mannosidase (Jack bean: Seikagaku Co.), α-L-fucosidase (bovine kidney: ProZyme, Inc.), or α-1- 2-L-fucosidase (*Corynebacterium* sp.: Takara Bio). PA-glycan was treated with the enzyme (50 mU) in 20 μl of 50 mM ammonium acetate buffer (β-galactosidase: pH 3.5, α-mannosidase and β-1–3 galactosidase: pH 4.5, α-2–3, -6 sialidase and β-*N*-acetylhexosaminidase: pH 5.0, α-2–3 sialidase and α-L-fucosidase: pH 5.5, and α-1–2-L-fucosidase: pH 8.5), at 37 °C for appropriate periods (0.5 h for α-2–3,-6 sialidase and α-2–3 sialidase; 20 h for others). The enzyme reaction was terminated by heating at 99.9 °C for 5 min.

Analysis of the Sialic Acid Linkage Type—The sialic acid linkage type was determined by its sensitivity to α-2–3, -6 sialidase (*Clostridium perfringens*: Merck) and α-2–3 sialidase (*Salmonella typhimurimum* LT2, recombinant, *Escherichia coli*: Takara Bio) treatment. Each acidic saccharide was treated with both sialidases, and the products were analyzed by anion-exchange HPLC using a Mono-Q column. If an acidic glycan has the α-2–3 type of Sia linkage, its retention time should decrease after digestion with both α-2–3, -6 and α-2–3 sialidases. In contrast, if the glycan has the α-2–6 type linkage, its retention time should be preserved after α-2–3 sialidase treatment. When all Sia residues are removed by the action of α-2–3, -6 sialidase, a neutral glycan should be generated.

RESULTS

Basic Strategy—Quantitative structural analysis of glycans from 201B7 (iPSC) and human dermal fibroblasts (SC)- A basic strategy for the construction of a comprehensive glycosylation "grand map" is shown in supplemental Fig. S1. Both *N*- and *O*-glycans were liberated from lyophilized iPSCs and SCs by gas-phase hydrazinolysis (22–25), and whole glycans comprising both intracellular (ER and Golgi) and surface membranous fractions were re-*N*-acetylated and labeled with 2-AP (26, 27). The derived PA-glycans were first separated by anion-exchange HPLC (supplemental Fig. S2*A*). Neutral glycans, which passed through the column (designated N fraction), and the adsorbed anionic glycans were fractionated and designated A1-A5 (according to the order of elution, supplemental Fig. S2*A*). The above fractions were then subjected to size-fractionation HPLC (for fractions N, A1 and A4, see supplemental Fig. S2*B*). When necessary, each fraction was further purified by reversed-phase HPLC (chromatogram not shown), and quantified on the basis of fluorescence intensity relative to an appropriate authentic standard (PA-Glc).

As regards neutral glycans, unambiguous assignment was made for glycans No.1–12, 14–26, and 29–30 by reversed-phase HPLC with MALDI-TOF MS confirmation. For others (*i.e.* 13, 27–28), serial exoglycosidase digestion was performed with β-galactosidase, β-1–3 galactosidase, β-*N*-acetylhexosaminidase, α-mannosidase, α-L-fucosidase and α-1–2-L-fucosidase, and the resultant products were identified via reversed-phase HPLC by comparison with samples of known structure. For example, a glycan fractionated as iPSC N-6–3 (No. 13) was treated with an α-fucosidase with broad specificity, and the retention time observed for the product agreed with that of M2B (glycan No.1), for which an authentic standard is available. As a result of these efforts, 27 *N*-linked glycans were identified as neutral glycans in iPSCs (Table I). Apparent contamination by high-molecular weight polyhexose was also observed in the iPSC N fraction, and attributed to components included in the medium used for iPSC preparation (data excluded from Table I). Likewise, 16 *N*-linked glycans were identified in SCs (Table I). In addition, *O*-linked glycans were analyzed under the conditions employed for hydrazinolysis (100 °C for 4 h) (details to be published elsewhere). From N fractions of iPSCs and SCs, 5- and 2- *O*-linked glycans were obtained, respectively (Table II).

Acidic glycans were further analyzed by a combination of sialidase digestion, MALDI-TOF MS and reversed-phase HPLC (supplemental Fig. S2). After digestion with universal α-2–3, -6 sialidase (*Clostridium perfringens*), the resultant products were passed through a Mono-Q column, analyzed by MALDI-TOF MS and reversed-phase HPLC, and their structures were determined as described above. The type of linkage of each sialic acid was determined by susceptibility to two sialidases, *i.e.* α-2–3-specific sialidase (cloned from *Salmonella typhimurimum* LT2 and expressed in *E. coli*) and the universal α-2–3, -6 sialidase from *C. perfringens*. As a result, 8 acidic *N*-linked glycans (No. 31–36, 39, 40) were identified in the iPSC A1 fraction, while 2 *N*-linked glycans (No. 37, 38) and 1 *O*-linked glycan (No. 53) were identified in the iPSC A4 fraction (Table I, II). Likewise, 2 *N*-linked glycans (No. 41, 42), and 2 *N*-linked glycans (No. 43, 44) and 1 *O*-linked glycan (No. 53) were identified in the SC A1 and A4 fractions, respectively (Table I, II). Notably, all of the acidic *N*-linked glycans derived from iPSCs had α-2–6-linked sialic acid, whereas those from SC had the α-2–3 linkage type (described later). On the other hand, no *N*-linked glycans were detected in substantial amounts (<1 pmol) in the A2, A3, or A5 fractions. Instead, 4 *O*-linked glycans (No. 50–52, 54) were identified in these fractions from both cell types (Table II). Although the five *O*-linked glycans included in the A2-A5 fractions (No.50–54) were common to iPSCs and SCs, the molar fraction (%) of the α-2–3 disialyl structure (No.53) was greatly reduced (from 11.5% to 1.4%) in iPSCs, whereas those of the other 4 sialoglycans remained largely the same (described below).

To confirm the reproducibility of the data obtained by structural analyses, two separate experiments were performed for both iPSCs and SCs using the same amounts of cell preparations. As a result, the obtained glycan values were largely the same. Moreover, individual values for various glycans agreed well between assays (supplemental Table S1). Indeed, sufficiently high correlation coefficients, *i.e.* 0.9846 and 0.9811, were obtained for iPSC and SC preparations, respectively (supplemental Fig. S3). Therefore, the data provided in this work assure a sufficiently high accuracy to permit discussion of the issue of a glycome shift from a quantitative viewpoint. Tables I and II provide details of the average yield of each glycan in iPSC and SC preparations.

TABLE I
List of N-linked glycans identified in SC and iPSC

No.	Structure	SC	iPSC
Pauci-mannose and High-mannose			
1		N-7-3[1] (5.0[2])	N-5-4 (3.5)
2		N-10-1 (0.4)	N-7-5 (0.3)
3	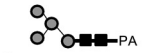	N-13-1 (0.4)	N-9-2 (0.4)
4	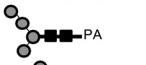		N-9-3 (0.5)
5	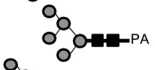	N-14-1 (0.6)	N-12-1 (5.6)
6		N-17-1 (13.0)	N-14-2 (8.9)
7	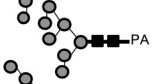	N-19-1 (5.4)	N-17-1 (6.9)
8		N-19-2 (3.6)	N-17-2 (2.8)
9	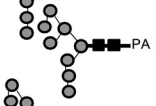	N-21-1 (14.3)	N-20-1 (17.6)
10		N-22-1 (14.2)	N-23-1 (20.8)
11		N-23-2 (0.4)	N-24-4 (4.2)
12	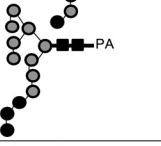		N-26-1 (2.5)
Fucosyl-pauci-mannose			
13		N-9-1 (10.8)	N-6-3 (9.3)
14	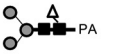	N-11-1 (1.8)	N-8-2 (2.8)

No.	Structure	SC	iPSC
Asialo complex			
15			N-8-3 (0.5)
16	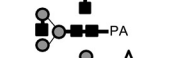		N-8-5 (0.4)
17			N-10-6 (0.5)
18			N-10-8 (0.8)
19	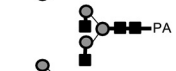		N-11-2 (0.4)
20			N-13-2 (0.5)
21			N-13-3 (0.7)
22			N-13-4 (0.9)
23			N-13-6 (0.3)
24		N-17-2 (13.2)	N-15-3 (0.4)
25		N-19-3 (4.5)	
26			N-15-5 (0.3)
27	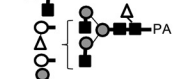		N-19-4 (0.7)
28			N-19-5 (0.6)
29	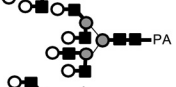	N-21-2 (0.7)	
30	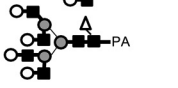	N-23-3 (0.4)	

No.	Structure	SC	iPSC
Sialylated complex			
31			A1-1 (0.5)
32			A1-4-1 (1.1)
33			A1-4-3 (0.5)
34			A1-6-3 (0.7)
35			A1-7-1 (1.0)
36			A1-7-3 (0.3)
37			A4-2-2 (0.6)
38			A4-2-3 (1.4)
39			A1-5-1 (0.3)
40	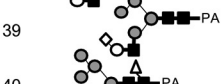		A1-6-2 (0.5)
41		A1-1-2 (1.9)	
42		A1-2-1 (2.7)	
43		A4-2-2 (1.5)	
44		A4-2-3 (5.2)	

[a] The hyphenated alphanumeric codes comprise fractionation procedures in the order of anion-exchange HPLC, size-fractionation HPLC and reversed-phase HPLC.

[b] The numbers in parentheses are the percentage as the total amount of *N*-linked glycans. Data are the average of two separate experiments.

Evidence for the Glycome Shift—Based on the above results, we noted the significant changes in *N*- and *O*-glycosylation patterns from SCs to iPSCs. Bar graph representations were made to compare molar fractions (%) of each glycan between the iPSC and SC fractions (Fig. 1). The data obtained are also summarized according to sub-categories of glycan structures presented in Fig. 2 (details described below).

High-mannose-type N-linked Glycans—Total amounts of high-mannose-type *N*-linked glycans were found to increase considerably in iPSCs (86.1% molar fraction) compared with SCs (69.9%) (Fig. 2). The significantly higher content of this type of glycan in iPSCs is represented by the presence of Man9 (No.10 in Table I) and Man5 (No.5). In contrast, complex-type *N*-linked glycans became less evident in iPSCs. Based on the presumed glycan synthetic pathways (30), these differences can likely be attributed to down-regulation of the expression of β-*N*-acetyl-glucosaminyltransferase I (MGAT1), which adds GlcNAc to Man5 as the first step in the biosynthesis of complex or hybrid-type glycans. It is also possible to speculate that Golgi α-mannosidase II is responsible for this structural change. In this regard, the expression of the MGAT1 gene was lowered 20-fold in iPSCs relative to SCs as shown in a previous DNA microarray analysis (21). If this is the case, it explains well why its substrate, Man5 (No.5), accumulates in iPSCs, while the levels of its downstream products (*i.e.* complex type glycans) decrease. On the other hand, we could not detect a significant level (>1 pmol) of the MGAT1 product, *i.e.* GlcNAcMan5, which is a substrate of the Golgi α-mannosidase II. Because this enzyme is specific to GlcNAcMan5 and its downstream products, but not to upstream products lacking GlcNAc, it is not clear whether Golgi α-mannosidase II is a

TABLE II
List of O-linked glycans identified in SC and iPSC

No.	Structure	SC	iPSC
Asialo			
45	PA	N-6-1[a] (9.9[b])	N-3-1 (10.9)
46	PA	N-7-1 (5.2)	N-5-2 (13.3)
47	PA		N-6-1 (3.9)
48	PA		N-7-2 (4.1)
49	PA		N-8-1 (9.6)
Sialylated			
50	PA	A2-2 (8.5)	A2-1 (9.1)
51	PA	A2-3 (14.2)	A2-2 (12.9)
52	PA	A3-1 (29.2)	A3-1 (24.3)
53	PA	A4-1-1 (11.5)	A4-1-1 (1.4)
54	PA	A5-1 (21.5)	A5-1 (10.5)

Gal GlcNAc Man Glc Fuc NeuAc — :α-linkage — :β-linkage

[a] The hyphenated alphanumeric codes consist of fractionation Procedures in the order of anion-exchange HPLC, size- fractionation HPLC, and reversed-phase HPLC.

[b] The numbers in parentheses are the percentage as the total amount of *O*-linked glycans. Data are the average of two separate experiments.

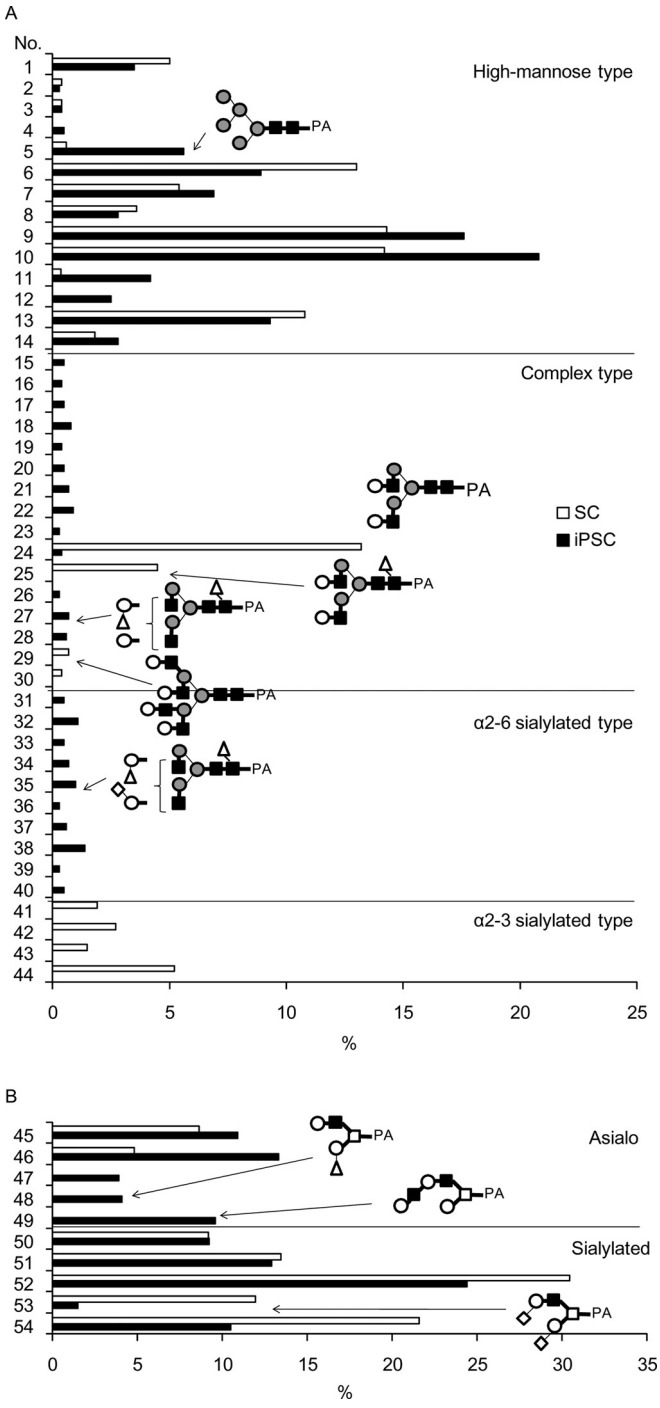

FIG. 1. **Comparison of (*A*) *N*-linked and (*B*) *O*-linked glycans prepared from iPSC and SC.** The yields of each glycan were expressed as percentages, taking the total amounts of *N*-linked or *O*-linked glycans prepared from each sample to be 100%. Glycan numbers correspond to those used in Tables I and II.

regulatory enzyme partaking in the observed change in high-mannose structures.

GlcNAc-exposed N-linked Glycans—The levels of GlcNAc-exposed complex type *N*-linked glycans (No. 15–23) were increased in iPSCs (5.3%), and essentially absent in SCs (Fig. 2, Table I). For this reason, a lowered expression of B4GALT, which transfers β-1–4-linked Gal to GlcNAc residues, is considered likely. In support of this, previous gene expression profiling showed a 15-fold decrease in B4GALT1, which is a major B4GALT in iPSCs (21). This explains the fact that a series of agalactosylated glycans with exposed GlcNAc (No. 15–23) are accumulated in iPSCs. On the other hand, sialylation appears to proceed immediately after full galactosylation occurs, because the proportion of sialylated complex-type glycans (6.9%) is much higher than that of fully galactosylated but non-sialylated glycans (1.7%). Taken together, these results lead to the conclusion that structures of complex type glycans of iPSCs are restricted to particular forms of sialoglycans (see below) in contrast to the strong depression of complex type glycan biosynthesis.

α-2–6 Sialylation—Sialylated *N*-linked glycans constituted 6.9% of the total *N*-linked glycans in iPSCs. Notably, the identified Sia- linkage was exclusively of the α-2–6 type (Table I and Fig. 2). This is in clear contrast to SCs, where sialylated *N*-linked glycans constituted 11.3% of the total

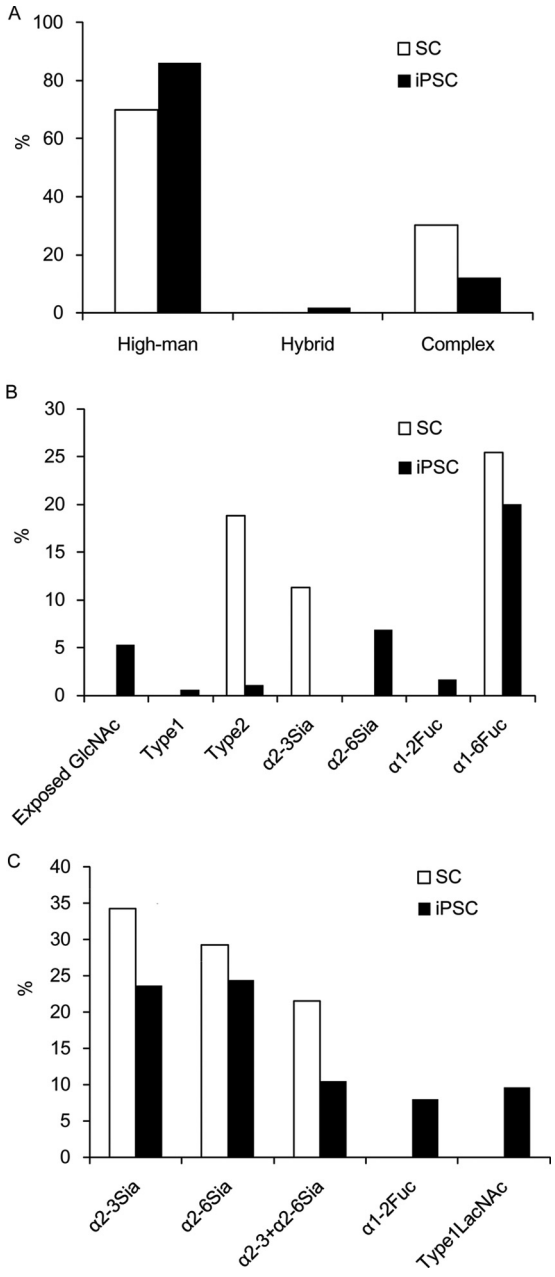

FIG. 2. **Alterations of epitopes of *N*- (A and B) or *O*-linked (C) glycans prepared from SC and iPSC.** These data were calculated based on the information provided in Tables I and II.

N-linked glycans, but were mostly of the α-2–3 type. Consequently, sialic acid in *N*-linked glycans of iPSCs was dramatically changed from the α-2–3 to the α-2–6 type, whereas total sialylation was reduced by 61%. Terminal features of iPSCs, including α-2–6 sialylation, are summarized in Table III along with their relation to previously reported lectin probes and glycosyltransferases (21).

Further to the above, essentially no α-2–3 Sia should be present in iPSCs with only α-2–6 linkage. To confirm this shift in Sia linkage, we analyzed total fractions containing Sia residues. In this way, unfractionated acidic fractions (iPSC A1-A5 and SC A1-A5) were treated with different types of sialidases, *i.e. C. perfringens* α-2–3, -6 and *S. typhimurimum* α-2–3 sialidases, and the resultant products were analyzed by anion-exchange HPLC (Fig. 3). When A1 and A4 fractions (corresponding to *N*-linked monosialylated and disialylated fractions, respectively) were treated with α-2–3 sialidase, almost all of the acidic glycans derived from the SC fractions were sensitive, indicating that they consist mostly of α-2–3 linked monosialylated (A1) and disialylated (A4) glycans, respectively. In contrast, the corresponding monosialylated (A1) fraction of iPSCs was substantially resistant to α-2–3 sialidase digestion. On the other hand, iPSC A4 gave two peaks corresponding to neutral and disialylated glycans after α-2–3 sialidase treatment. Therefore, it is evident that iPSC A1 exclusively consists of α-2–6 linked monosialylated glycans, whereas iPSC A4 consists of a majority of α-2–6 linked disialylated glycans with a small amount of α-2–3 linked disialylated glycans. The latter corresponds to an α-2–3 linked disialylated *O*-glycan (No.53 in Table II). In support of this observation, previous lectin microarray analysis showed a considerable increase in α-2–6 sialylation upon induction of pluripotency (21). DNA microarray analysis also supports the up-regulated expression of CMP-NeuAc:galactoside alpha-2,6-sialyltransferase 1 (ST6Gal1) and CMP-NeuAc:galactoside alpha-2,6-sialyltransferase 2 (ST6Gal2) in iPCSs. All of these observations unambiguously demonstrate that the linkage type of sialic acid in *N*-glycans is changed to the α-2–6 type upon undifferentiation.

Sialidase analysis of other acidic fractions suggested that A2, A3 (monosialo-), and A5 (disialo-) fractions correspond to *O*-linked glycans No. 51, 52, and 54, respectively (Table II). However, the difference in the linkage type of sialic acid in *O*-linked glycans between iPSCs and SCs was relatively small except for that of No.53. Nevertheless, the total content of acidic *O*-linked glycans was lower in iPSCs (58.2%) compared with that of SCs (84.9%).

α-1–2 Fucosylation—Significant amounts of α-1–2 linked fucose were found in both *N*- (1.7%) and *O*-linked glycans (8.0%) from iPSCs, while none were detected in SCs. This finding agrees well with the results obtained by previous lectin microarray analysis, and with the up-regulated expression of the two fucosyltransferases responsible for α-1–2 fucosylation, FUT1 and FUT2 (21) (see also Table III).

Two α-1–2 fucosylated *N*-linked glycans (No.27 and No.35) were identified in iPSCs: briefly, a glycan fractionated as iPSC N-19–4 corresponded to difucosylated biantennary glycan (*m/z*, 2033.6 $[M+Na]^+$ in positive ion mode) in MALDI-TOF MS. This glycan was treated with α-1–2 fucosidase and an α-fucosidase with broad specificity. As a result, the retention times observed for the products agreed with those of core-fucosylated and non-fucosylated biantennary glycans, respectively (supplemental Fig. S4). Thus, iPSC N-19–4 was identified as α-1–2 and core-fucosylated biantennary glycan

TABLE III

Typical features of pluripotency-related glycan structures, and relation of glycan ligands to corresponding lectin probes and glycosyltransferase genes

Terminal structure[a]		Typical structure[a]	Glycan No.	Lectin probe[b]	Glycotransferease[c]
Sia	α2-6	*N*-glycan	31-40	SNA SSA TJAI rPSL1a	ST6GAL1 ST6GAL2
Fuc	α1-2	*N*-glycan	27, 35	rGC2 rBC2LCN	FUT1 FUT2
		O-glycan	47, 48		
LacNAc linkage	β1-3	*N*-glycan	28	BPL	B3GALT5
		O-glycan	49		

[a] For definition of structural descriptions, see legends to Table I.

[b] Lectins effective for probing the presence of depicted glycosylation features or glycan ligands. Data from ref. (21).

[c] Glycosyltransferase genes, of which over-expressions are responsible for the depicted glycan structures Data from ref. (21).

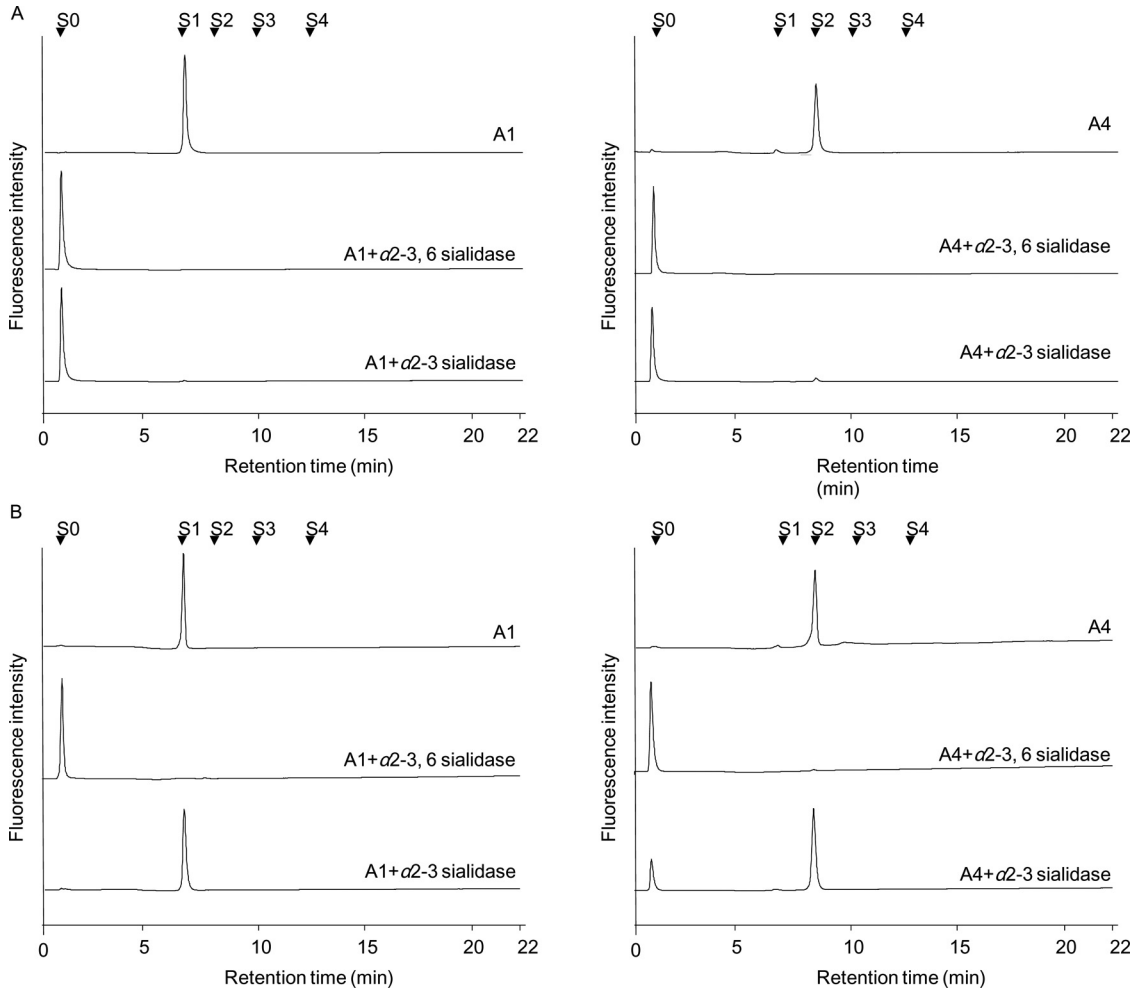

FIG. 3. **Analysis of the linking mode of sialic acid contained in iPSC and SC acidic fractions.** Each iPSC A1, A4, SC A1, and A4 fraction was treated with α-2–3, -6 sialidase and α-2–3 sialidase, and the reaction mixtures were analyzed by anion-exchange HPLC as described in "Experimental procedures." S0, S1, S2, and S3 are standard glycans binding sialic acid.

(No.27). Likewise, a glycan fractionated as iPSC A1–7-1 (No.35) was identified as α-1–2 and core-fucosylated, and α-2–6 monosialylated biantennary glycan (Table I). In contrast, no α-1–2 fucosylated *N*-linked glycan was detected in SCs.

Two fucosylated *O*-linked glycans were detected in iPSC N-6–1 (No.47) and N-7–2 (No.48) fractions (Table II). They gave the same *m/z* value (973.4 $[M+H]^+$ in positive ion mode) corresponding to a fucosyl Gal-core 2 structure in MALDI-TOF MS, and their retention times shifted to that of Gal-core 2 (No.46) after treatment with α-1–2 fucosidase. However, only No. 47 was sensitive to the digestion with β-1–3 galactosidase. Therefore, structures of N-6–1 (No.47) and N-7–2 (No.48) were considered to be Fuc-α-1–2Gal-β-1–4GlcNAc-β-1–6(Gal-β-1–3)GalNAc and Gal-β-1–4GlcNAc-β-1–6(Fuc-α-1–2Gal-β-1–3)GalNAc, respectively (Table II).

Thus, we conclude that α-1–2 linked fucose is a critical epitope to characterize iPSCs. On the other hand, a decrease in core-fucosylation from 25.4% to 20.0% was rather moderate (Fig. 2).

Type 1 LacNAc—The final feature characteristic of iPSCs is the emergence of the type 1 LacNAc structure. In the present study, a triantennary *N*-linked glycan (*m/z*, 2084.8 $[M+H]^+$, 0.6% of the total *N*-linked glycans) was derived from iPSC N-19–5, of which the retention time agreed with an authentic standard (No.28, Table I). The presence of a single Gal-β-1–3 residue was confirmed by β-1–3 galactosidase digestion.

An *O*-linked glycan, iPSC N-8–1 (*m/z*, 1192.5 $[M+H]^+$), was also sensitive to β-1–3 galactosidase, and the most probable structure was proposed (No. 49, Table II). The emergence of type 1 LacNAc (No. 49) in *O*-glycans was quite remarkable from a quantitative viewpoint, because such glycans were not detected at all in SCs, while the absolute amount of this glycan was as high as 9.6% of the total *O*-glycans (also compare with the *N*-glycan No. 28 described above). As an explanation for this, the increased expression of B3GalT5, which is the major B3GalT involved in the synthesis of type 1 LacNAc, was observed in human iPSCs and ESCs relative to SCs (21) (also see Table III). Notably, this enzyme is also involved in the synthesis of the glycolipid-type pluripotency glyco-markers SSEA3 and SSEA4 (18, 21). Therefore, it is possible to speculate that B3GalT5 is a key enzyme in the synthesis of these pluripotency-related glycan markers.

Based on the above structural analysis of glycoprotein glycans both from iPSCs and SCs as well as on their quantitative data, the global features of the dynamic glycome shift upon undifferentiation can be understood in terms of a "grand map" (Fig. 4).

DISCUSSION

For structural glycomics, two different approaches have been taken thus far: mass spectrometry (MS) (17) and lectin microarray (18–20, 21). However, neither of these is sufficiently quantitative nor reliably comparative for the purpose of drawing a "grand map" of glycoprotein glycans from iPSCs and SCs. A recent study focusing on enriched plasma membrane of hESCs succeeded in part in revealing a glycome shift. Unfortunately, the observed change was restricted to the major group of *N*-glycans, *i.e.* high-mannose-type glycans, which represent immature biosynthesis products of *N*-glycans (31). On the other hand, the present study targeted whole cell extracts, and provides various lines of evidence in support of a "glycome shift" across a wider dynamic range. Interpretation of the results clearly reveals the strong tendency to suppress the biosynthesis of complex-type *N*-glycans (Fig. 4): a series of high-mannose type glycans became evident in iPSCs (Fig. 2), which is attributed to the down-regulation of relevant ER α-mannosidases and subsequent β-*N*-acetyl-glucosaminyltransferase (GnT) I. Together with accumulation of the resultant Man5, a key structure to complex type maturation, the biosynthesis of downstream products was further depressed by the down-regulation of β-1–4-GalT (21). All these events seem to set up a "prerequisite" stage before cells become undifferentiated and acquire pluripotency.

More critically, however, significant structural changes have been observed in the outermost domains of glycans in terms of α-2–6 sialylation, H-type fucosylation, and type 1 LacNAc structure (Fig. 2). Some *N*- and *O*-linked glycans in iPSCs have α-1–2 linked fucose, but no such glycans were detected in SCs. Another impressive feature of iPSCs is the emergence of type 1 LacNAc structures both in *N*- and *O*-linked glycans (No. 28 and 49, respectively). Notably, glycan 49 corresponds to an epitope structure recognized by Tra-1–60/81 in a recent report (11). Because the type 1 LacNAc is produced by β-1–3-GalT, this is likely to be a key enzyme relevant to pluripotency, in addition to ST6Gal and FUT1/2. Interestingly, all of the structural features determined in the present study are in good agreement with our previous data (21) obtained by lectin microarray and gene expression analyses (Table III).

Although the biological significance of the present findings remain largely elusive, some speculation is possible. A linkage shift from α-2–3 to α-2–6 may affect the biological functions of endogenous lectins. Galectins, a group of soluble β-galactoside-binding lectins exhibit no or greatly diminished binding to β-galactosides (*e.g.* LacNAc) when capped with α-2–6 linked sialic acid (32, 33). In this context, it is worth mentioning that ST6Gal 1 is over-expressed in many types of human cancers, which led to the hypothesis that tumor cells are protected against galectin-mediated apoptosis via α-2–6 sialylation of surface receptors (34).

Fucosylation is also involved in many cell adhesion and signaling events (35, 36). The published gene expression profiles have demonstrated that the α-1–2 fucosyltransferase gene FUT1 is overexpressed in hESCs compared with embryoid body. In addition, FUT2, FUT4, and FUT8, encoding α-1–2, α-1–3, and α-1–6 fucosyltransferase enzymes, respectively, are expressed in hESC (17). In our previous study, we showed that

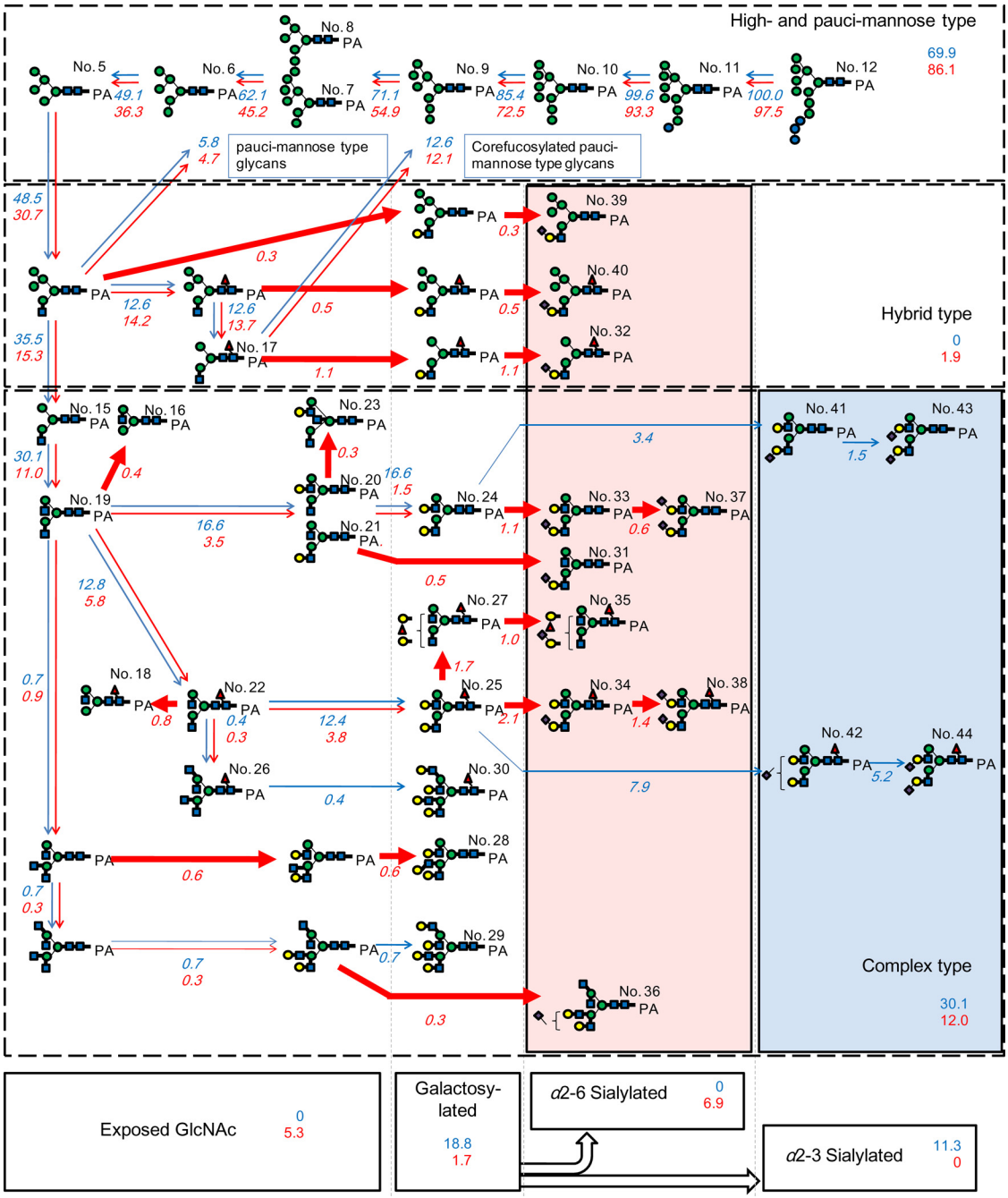

FIG. 4. **A glycome "grand map" covering presumed biosynthetic pathways of *N*-linked glycans produced in iPSCs and SCs.** Glycan numbers (1–44) correspond to those defined in Table I. The map is constructed based on the generally accepted biosynthetic pathways of *N*-linked glycans (30). Red and blue arrows indicate biosynthetic reactions depicted in iPSCs and SCs, respectively. Estimated percentages of respective biosynthetic reactions are shown in *italicized* figures near the arrows, where the starting precursor Man9Glc3GlcNAc2 (No. 12, 100%) is taken as 100%. Quantitative data are from Table I. Thick arrows indicate specific reactions exclusively detected in iPSCs. The following monosaccharide symbols are used to express glycan structures: *green* circle, Man; *blue* square, GlcNAc; *yellow* circle, Gal; *blue* circle, Glc; *red* triangle, Fuc; *violet* diamond, NeuAc.

FUT1 and FUT2 are overexpressed in iPSCs, but that FUT8 expression is decreased compared with SCs (21). Notably, stem cell specific overexpression of FUT1 correlates well with our finding that more complex fucosylation takes place in *N*-linked glycans of iPSCs. FUT2 expressed in stem cells is considered to be responsible for the α-1–2 fucosylation of *O*-linked glycans based on its preference for type 1, 3, and 4 chains, which were scarcely detected in *N*-linked glycans in the present study. The decreased expression of FUT8 in iPSCs is consistent with the decreased core-fucosylation.

Recently, Tang and co-workers reported a monoclonal antibody raised against human pluripotent stem cells (hPSCs), including hESCs and human iPSCs (37). Interestingly, this antibody, designated SSEA-5 was shown to specifically bind to the H type 1 glycan, Fuc-α-1–2-Gal-β-1–3-GlcNAc. This epitope coincides with the glycan structure recognized by a lectin, rBC2LCN, which was found to be the best probe lectin to evaluate the pluripotency of iPSCs and ESCs (21). In this respect, using an advanced lectin microarray technique called the "antibody-overlay method," we have recently identified podocalyxin as a likely glycoprotein carrying rBC2LCN glycan ligands (Tateno *et al.*, unpublished results). Moreover, rBC2LCN was found to show substantial affinity to α-1–2 fucosylated type 1 (Gal-β1–3GlcNAc) and type 3 (Gall-β1–3GalNAc) glycan structures. In effect, an *O*-glycan (No. 48) corresponding to the latter has been identified in the present study. Although biological functions of these type 1/3 H glycans remain to be elucidated, their possible involvement in pluripotency *via* homophilic carbohydrate-carbohydrate interaction is feasible, as has been identified in compaction at the morula stage of F9 embryonal carcinoma cells (38). On the other hand, expression of the ABO gene was low in our gene microarray analysis in which more than 100 iPSCs derived from six different cell types were tested (Tateno *et al.*, unpublished results). This observation implies that the undifferentiation process involves neither A nor B blood group biosynthesis. To this extent, it is not known at all whether Bombay type (H^-/H^-) individuals can produce iPSCs with similar efficiency to normal individuals. Further study is necessary to examine these hypotheses concerning glycan functions in pluripotency.

In conclusion, of particular note are the α-2–6 sialylation, α-1–2 fucosylation and type 1 LacNAc characteristics identified here, which are specific to iPSCs. Although the functions of these modifications remain unclear, one key experiment to solve this question is to characterize glycoproteins carrying rBC2LCN glycan ligands, which include podocalyxin. The present observations provide strong focus and direction for future stem cell biology research.

Acknowledgments—We thank Ms. Asako Matsushima, Mr. Yasuhiko Aiki, and Ms. Kumiko Higuchi for help with the preparation of cell cultures. This work was supported by the New Energy and Industrial Technology Development Organization (NEDO) of Japan. Human iPS cells (201B7) were obtained from RIKEN Bioresource Center.

*

Ⓢ This article contains supplemental Figs. S1 to S4 and Table S1.

¶ To whom correspondence should be addressed: Research Center for Stem Cell Engineering, National Institute of Advanced Industrial Science and Technology (AIST), Central 2, 1–1-1 Umezono, Tsukuba, Ibaraki 305-8568, Japan. Tel.: +81-29-861-3125; E-mail address: jun-hirabayashi@aist.go.jp.

REFERENCES

1. Takahashi, K., and Yamanaka, S. (2006) Induction of pluripotent stem cells from mouse embryonic and adult fibroblast cultures by defined factors. *Cell* **126,** 663–676
2. Takahashi, K., Tanabe, K., Ohnuki, M., Narita, M., Ichisaka, T., Tomoda, K., and Yamanaka, S. (2007) Induction of pluripotent stem cells from adult human fibroblasts by defined factors. *Cell* **131,** 861–872
3. Yu, J., Vodyanik, M. A., Smuga-Otto, K., Antosiewicz-Bourget, J., Frane, J. L., Tian, S., Nie, J., Jonsdottir, G. A., Ruotti, V., Stewart, R., Slukvin, I. I., and Thomson, J. A. (2007) Induced pluripotent stem cell lines derived from human somatic cells. *Science* **318,** 1917–1920
4. Hanna, J., Wering, M., Markoulaki, S., Sun, C. W., Meissner, A., Cassady, J. P., Beard, C., Brambrink, T., Wu, L. C., Townes, T. M., and Jaenisch, R. (2007) Treatment of sickle cell anemia mouse model with iPS cells generated from autologous skin. *Science* **318,** 1920–1923
5. Viczian, A. S., Solessio, E. C., Lyou, Y., and Zuber, M. E. (2009) Generation of functional eyes from pluripotent cells. *PLoS Biol.* **7,** e1000174
6. Inoue, H., and Yamanaka, S. (2011) The use of induced pluripotent stem cells in drug development. *Clin. Pharmacol. Ther.* **89,** 655–661
7. Rashid, S. T., Corbineau, S., Hannan, N., Marciniak, S. J., Miranda, E., Alexander, G., Huang-Doran, I., Griffin, J., Ahrlund-Richter, L., Skepper, J., Semple, R., Weber, A., Lomas, D. A., and Vallier, L. (2010) Modeling inherited metabolic disorders of the liver using human induced pluripotent stem cells. *J. Clin. Invest.* **120,** 3127–3136
8. Varki, A., and Lowe, J. B. (2009) Biological roles on glycans. *Essentials of Glycobiology*: 2nd Ed., 75–88, Cold Spring Harbor Laboratory, NY, Cold Spring Harbor Laboratory Press, Plainview, NY
9. Muramatsu, T., and Muramatsu, H. (2004) Carbohydrate antigens expressed on stem cells and early embryonic cells. *Glycoconj. J.* **21,** 41–45
10. Schopperle, W. M., and DeWolf, W. C. (2007) The TRA-1–60 and TRA-1–81 human pluripotent stem cell markers are expressed on podocalyxin in embryonal carcinoma. *Stem Cells* **25,** 723–730
11. Natunen, S., Satomaa, T., Pitkanen, V., Salo, H., Mikkola, M., Natunen, J., Otonkoski, T., and Valmu, L. (2011) The binding specificity of the marker antibodies Tra-1–60 and Tra-1–81 reveals a novel pluripotency associated type 1 lactosamine epitope. *Glycobiology* **21,** 1125–1130
12. Lanctot, P. M., Gage, F. H., and Varki, A. P. (2007) The glycans of stem cells. *Curr. Opin. Chem. Biol.* **11,** 373–380
13. Kobata, A. (1992) Structures and functions of the sugar chains of glycoproteins. *Eur. J. Biochem.* **209,** 483–501
14. Varki, A. (1993) Biological roles of oligosaccharides: all of the theories are correct. *Glycobiology* **3,** 97–130
15. Dennis, J. W., Granovsky, M., and Warren, C. E. (1999) Glycoprotein glycosylation and cancer progression. *Biochim. Biophys. Acta* **1473,** 21–34
16. Karlsson, K. A. (1998) Meaning and therapeutic potential of microbial recognition of host glycoconjugates. *Mol. Microbiol.* **29,** 1–11
17. Satomaa, T., Heiskanen, A., Mikkola, M., Olsson, C., Blomqvist, M., Tiittanen, M., Jaatinen, T., Aitio, O., Olonen, A., Helin, J., Hiltunen, J., Natunen, J., Tuuri, T., Otonkoski, T., Saarinen, J., and Laine, J. (2009) The *N*-glycome of human embryonic stem cells. *BMC Cell Biol.* **10,** 42
18. Saito, S., Onuma, Y., Ito, Y., Tateno, H., Toyoda, M., Hidenori, A., Nishino, K., Chikazawa, E., Fukawatase, Y., Miyagawa, Y., Okita, H., Kiyokawa, N., Shimma, Y., Umezawa, A., Hirabayashi, J., Horimoto, K., and Asashima, M. (2011) Possible linkages between the inner and outer cellular states of human induced pluripotent stem cells. *BMC Syst. Biol.* **20,** 5
19. Toyoda, M., Yamazaki-Inoue, M., Itakura, Y., Kuno, A., Ogawa, T., Yamada, M., Akutsu, H., Takahashi, Y., Kanzaki, S., Narimatsu, H., Hirabayashi, J., and Umezawa, A. (2011) Lectin microarray analysis of pluripotent and multipotent stem cells. *Genes Cells.* **16,** 1–11
20. Wang, Y. C., Nakagawa, M., Garitaonandia, I., Slavin, I., Altun, G., Lacharite, R. M., Nazor, K. L., Tran, H. T., Lynch, C. L., Leonardo, T. R., Liu, Y., Peterson, S. E., Laurent, L. C., Yamanaka, S., and Loring, J. F. (2011) Specific lectin biomarkers for isolation of human pluripotent stem cells identified through array-based glycomic analysis. *Cell Res.* **21,** 1551–1563
21. Tateno, H., Toyota, M., Saito, S., Onuma, Y., Ito, Y., Hiemori, K., Fukumura, M., Matsushima, A., Nakanishi, M., Ohnuma, K., Akutsu, H., Umezawa, A., Horimoto, K., Hirabayashi, J., and Asashima, M. (2011) Glycome diagnosis of human induced pluripotent stem cells using lectin microarray. *J. Biol. Chem.* **286,** 20345–20353
22. Takasaki, S., Mizuochi, T., and Kobata, A. (1982) Hydrazinolysis of asparagine-linked sugar chains to produce free oligosaccharides. *Methods*

Enzymol. **83,** 263–268
23. Kawashima, H., Murata, T., Yamamoto, K., Tateishi, A., Irimura, T., and Osawa, T. (1992) A simple method for the release of asparagine-linked oligosaccharides from a glycoprotein purified by SDS-polyacrylamide gel electrophoresis. *J. Biochem.* **111,** 620–622
24. Kaku, H., Mori, Y., Goldstein, I. J., and Shibuya, N. (1993) Monomeric, monovalent derivative of Maackia amurensis leukoagglutinin. Preparation and application to the study of cell surface glycoconjugates by flow cytometry. *J. Biol. Chem.* **268,** 13237–132341
25. Hasui, Y., Fukui, Y., Kikushi, J., Kato, N., Miyairi, K., and Okuno, T. (1998) Isolation, Characterization, and Sugar Chain Structure of EndoPG Ia, Ib, and Ic from *Stereum purpureum. Biosci. Biotechnol. Biochem.* **62,** 852–857
26. Hase, S., Ikenaka, T., and Matsushima, Y. (1978) Structure analyses of oligosaccharides by tagging of the reducing end sugars with a fluorescent compound. *Biochem. Biophys. Res. Commun.* **85,** 257–263
27. Hase, S. (1994) High-performance liquid chromatography of pyridylaminated saccharides. *Methods Enzymol.* **230,** 225–237
28. Tokugawa, K., Oguri, S., and Takeuchi, M. (1996) Large scale preparation of PA-oligosaccharides from glycoproteins using an improved extraction method. *Glycoconj. J.* **13,** 53–56
29. Natsuka, S., Adachi, J., Kawaguchi, M., Ichikawa, A., and Ikura, K. (2002) Method for purification of fluorescence-labeled oligosaccharides by pyridylamination. *Biosci. Biotechnol. Biochem.* **66,** 1174–1175
30. Stanley, P., Schachter, H., and Taniguchi, N. (2009) N-Glycans. *Essentials of Glycobiology*: 2nd Ed., 101–114, Cold Spring Harbor Laboratory, NY
31. An, H. J., Gip, P., Kim, J., Wu, S., Park, K. W., McVaugh, C. T., Schaffer, D. V., Bertozzi, C. R., and Lebrilla, C. B. (2012) Extensive determination of glycan heterogeneity reveals an unusual abundance of high mannose glycans in enriched plasma membranes of human embryonic stem cells. *Mol. Cell. Proteomics.* **11,** M111.010660
32. Hirabayashi, J., Hashidate, T., Arata, Y., Nishi, N., Nakamura, T., Hirashima, M., Urashima, T., Oka, T., Futai, M., Muller, W. E., Yagi, F., and Kasai, K. (2002) Oligosaccharide specificity of galectins: a search by frontal affinity chromatography. *Biochim Biophys Acta* **1572,** 232–254
33. Iwaki, J., Tateno, H., Nishi, N., Minamisawa, T., Nakamura-Tsuruta, S., Itakura, Y., Kominami, J., Urashima, T., Nakamura, T., and Hirabayashi, J. (2011) The Galβ-(syn)-gauche configuration is required for galectin-recognition disaccharides. *Biochim. Biophys. Acta* **1810,** 643–651
34. Zhuo, Y., Chammas, R., and Bellis, S. L. (2008) Sialylation of beta1 integrins blocks cell adhesion to galectin-3 and protects cells against galectin-3-induced apoptosis. *J. Biol. Chem.* **283,** 22177–22185
35. Staudacher, E., Altmann, F., Wilson, I. B., and März, L. (1999) Fucose in *N*-glycans: from plant to man. *Biochim. Biophys. Acta* **1473,** 216–236
36. Becker, D. J., and Lowe, J. B. (2003) Fucose: biosynthesis and biological function in mammals. *Glycobiology* **13,** 41R–53R
37. Tang, C., Lee, A. S., Volkmer, J. P., Sahoo, D., Nag, D., Mosley, A. R., Inlay, M. A., Ardehali, R., Chavez, S. L., Pera, R. R., Behr, B., Wu, J. C., Weissman, I. L., abd Drukker, M. (2011) An antibody against SSEA-5 glycan on human pluripotent stem cells enables removal of teratoma-forming cells. *Nat. Biotechnol.* **14,** 829–834
38. Eggens, I., Fenderson, B., Toyokuni, T., Dean, B., Stroud, M., and Hakomori, S. (1989) Specific interaction between Le^x and Le^x determinants. A possible basis for cell recognition in preimplantation embryos and in embryonal carcinoma cells. *J. Biol. Chem.* **264,** 9476–9484